Journal of the European Ceramic Society 20 (2000) 2169–2174

Mechanical alloying of alumina–yttria powder mixtures

J. Alkebro [a,b,*], S. Begin-Colin [b], A. Mocellin [b], R. Warren [a]

[a] *Division of Engineering Materials, Luleå University of Technology, SE-971 87 Luleå, Sweden*
[b] *Laboratoire de Sciences et Génie des Matériaux Métalliques, UMR CNRS 7584, Ecole des Mines de Nancy, Parc de Saurupt, F-54042 Nancy Cedex, France*

Received 11 October 1999; received in revised form 7 February 2000; accepted 12 February 2000

Abstract

Mechanical alloying has been used to prepare powder mixtures of alumina and yttria as a means to create composites with a dominant matrix phase together with small particles of a dispersed second phase. The yttria–alumina system, containing five possible phases, has the potential for creating eight combinations of matrix and dispersed phases. Here compositions designed to give $YAlO_3$ (YA) dispersed in $Y_3Al_5O_{12}$ (Y_3A_5 i.e. YAG) or $Y_4Al_2O_9$ (Y_2A) were studied. After milling with steel tools for times up to 8 h, the powders were subjected to thermal cycles up to 1500°C during which the phase evolution was monitored using X-ray diffractometry (including high-temperature XRD) and differential thermal analysis. During milling the original crystal structures were quickly broken down, in some cases partially replaced by an intermediate structure after milling. Upon subsequent heating the milled mixtures crystallized to give the expected phases, YA in Y_3A_5 and YA in Y_2A respectively, but the reaction route was seen to be different depending on the amount of amorphization of the yttria. Contamination by iron was seen to affect the phase distribution and the lattice parameters.

Keywords: Al_2O_3–Y_2O_3; Mechanical alloying; Milling; Phase evolution; Thermal properties

1. Introduction

Dispersion of fine particles in a matrix material has been shown to have a positive effect on fracture toughness and creep properties for some materials, for instance SiC in alumina.[1] However, for very high temperatures in oxidizing atmospheres it is often more suitable to use oxides throughout the structure to ensure the stability of the material. A possible way of obtaining the desired microstructure using oxides only, is to use the neighboring phases in an oxide–oxide system in equilibrium. One of the phases is selected as the matrix, while the second phase is dispersed in the system, thus creating the desired microstructure. The alumina-yttria system, which has several intermediate phases that can be combined,[2] seems suitable for this purpose, and the use of mechanical alloying for treating powders before sintering is proposed as a preparation method. This method has been shown[3] to produce very fine nanocrystalline particles when used on oxide materials, and it is expected to allow for a good dispersion of the second phase. Earlier work on polycrystals in this system has mainly focused on alumina rich compositions prepared using sol-gel methods [4] or wet milling of powders.

The alumina-yttria system is not very well known, but it is believed to have three intermediate phases:[2] $Y_3Al_5O_{12}$, $YAlO_3$ and $Y_4Al_2O_9$. Based on the behavior of the system under some circumstances, a metastable phase diagram has been constructed where $Y_3Al_5O_{12}$ is missing.[5–8] There has been some argument about the stability and properties at the melting point of some of the intermediate phases,[6–13] but the latest findings suggest that all three intermediate phases are sufficiently stable. There is no solid solution reported within the binary system.

The phases are here labeled according to the proposal of Cockayne,[2] denoting alumina as A and yttria as Y, giving the intermediate phases Y_3A_5 ($Y_3Al_5O_{12}$ or YAG), YA ($YAlO_3$ or YAP) and Y_2A ($Y_4Al_2O_9$ or YAM).

2. Experimental

The starting materials for this study were high-purity alumina (from Martinswerk) and yttria (from SEPR)

* Corresponding author.
E-mail address: jesper.alkebro@mb.luth.se (J. Alkebro).

0955-2219/00/$ - see front matter
PII: S0955-2219(00)00073-X

powders. Two mixtures of these powders were investigated, mixture 1 consisting of 37.9 wt% alumina and 62.1 wt% yttria (57.5 and 42.5 at% respectively), and mixture 2 consisting of 21.9 wt% alumina and 78.1 wt% yttria (38.3 and 61.7 at% respectively). These compositions, indicated in Fig. 1, correspond to the expected dispersion of 40 vol% YA in Y_3A_5 and 30 vol% YA in Y_2A. The mixtures were milled in a planetary ball mill (Fritsch Pulverisette 7) using steel vials and balls in air. The powder to ball weight ratio was 1/40. The milled powders were examined in differential thermal analysis (DTA) and X-ray diffraction (XRD) (before and after DTA) using CoK_α radiation ($\lambda = 0.178\ 897$ nm). DTA was performed in Ar heating to 1500°C at 20°C/min followed by cooling at 30°C/min. The cycle was repeated once to allow for correction of equipment related features in the diagram. Before XRD 20 wt% Si-powder was added as an internal standard.

Finally, to gain a better understanding of the processes occurring in the milled powders during heat treatment, some of the samples were examined by high-temperature X-ray diffraction (HTXRD) in air using CuK_α radiation ($\lambda = 0.154\ 060$ nm). Heating during HTXRD was 10°C/min, and the scans took 15 min. Curve fitting was performed on XRD data using Philips Profile Fit software.

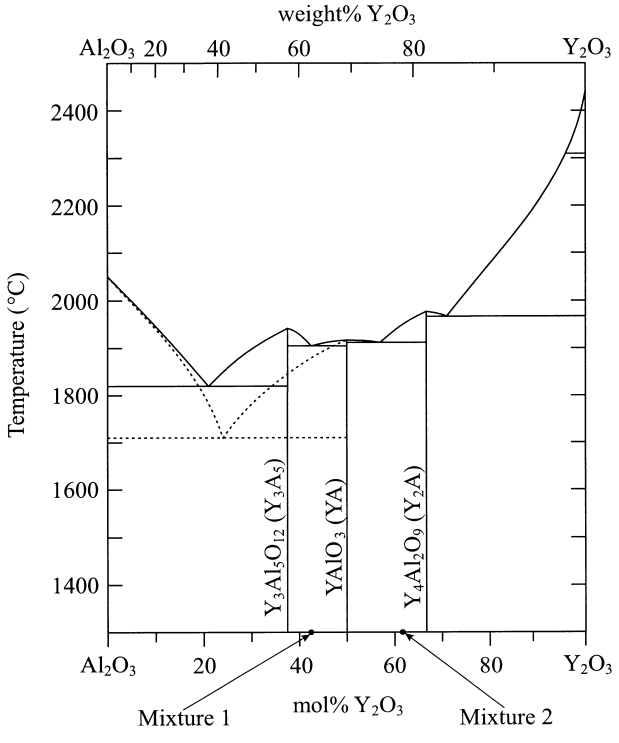

Fig. 1. The Al_2O_3–Y_2O_3 system with the compositions of the examined samples. Solid lines represent equilibrium phases after Adylov et al.,[11] and dashed lines show metastable phase relations after Lakiza et al.[5]

3. Results

The milling balls were found to be the major source of iron contamination during milling. Weight loss of the balls ranged between 0.06 and 0.37 g for milling times of 0.5–8 h respectively, the weight of the balls being 116 g. In addition weight loss from the vials is often about 20–40% of the loss of the balls. However, the weight loss was measured after cleaning and so somewhat overestimates the amount entering the sample.

The XRD peaks of the original yttria structure lose intensity very rapidly during milling, as can be seen in Fig. 2, and they are completely gone after 4 h of milling. The alumina structure seems to be somewhat more resistant to milling, and there are still signs of its peaks after 8 h of milling. However, in the interval between 33 and 40° (2θ angle, CoK_α radiation) a new set of broad low-intensity peaks appear, these being the most pronounced after 2 h of milling. If the milling is continued, these new peaks broaden and turn into a wide area of heightened intensity as for an amorphous material.

DTA indicates a dramatic change in the reactions of the powders depending on the milling. For powders milled a short time, the DTA graph is fairly featureless, but after being milled 4 h or more, an exothermic peak appears at 900°C. Additional investigation of mixture 2 in HTXRD shows that the reactions in the powder take different routes. For short milling times yttria is seen to recrystallize to cubic yttria starting at 400°C and continuing up to 1250°C, where there is a shift to the intermediate phases. For longer milling times (and, therefore, more broken up crystal structures) there are no signs of diffraction peaks up to 800°C, where the intermediate phases start to form directly from the amorphous material. XRD after DTA reveals that the milled samples have been entirely transformed to the expected intermediate phases predicted by the phase diagram i.e. YA and Y_3A_5 for mixture 1 and YA and Y_2A for mixture 2. Non-milled samples of both mixtures exhibited an incomplete reaction, containing all the phases in the alumina-yttria system after DTA.

As the XRD peaks overlap significantly, a selection of suitable peaks with least overlap was chosen for curve fitting. The change in the ratio of the peak areas is considered to be roughly equivalent to the change in the weight ratio of the phases. As can be seen in Fig. 4, for mixture 1 the amount of YA falls continuously with increasing milling time, whereas in mixture 2 the amount of YA rises at first and then remains fairly stable.

There is a noticeable shift in the 2-theta values of the intermediate phases depending on the milling time. The angles derived by means of curve fitting enabled the estimation of the change in plane spacing corresponding to this shift. Looking at Figs. 5 and 6, the spacing of investigated planes of Y_3A_5 and YA increased with

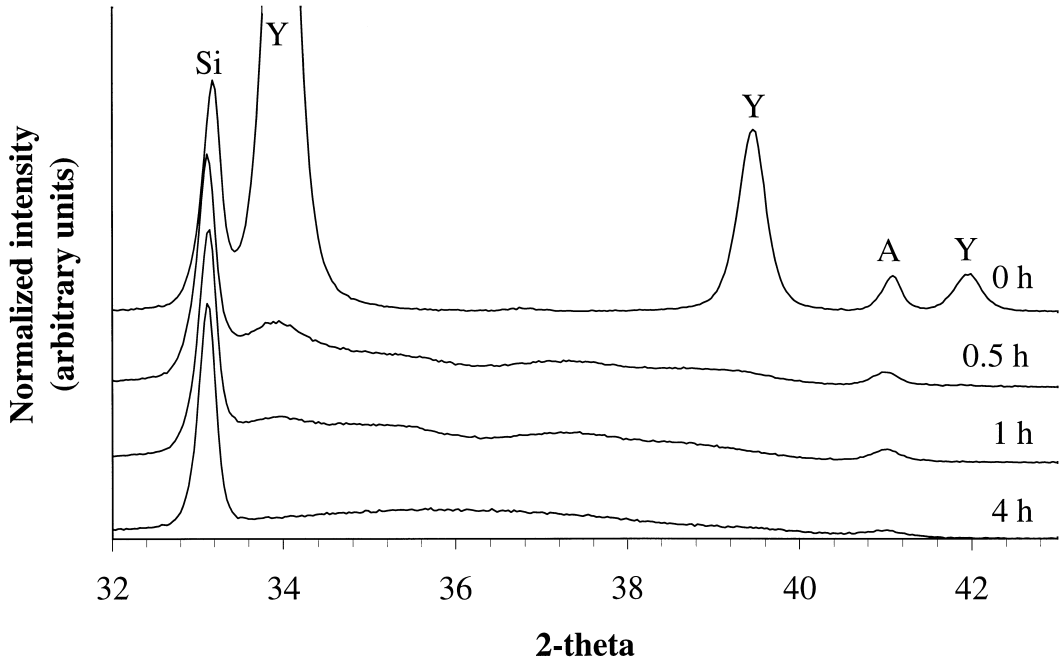

Fig. 2. As-milled XRD of mixture 2. The intensities are normalized to be equal at the Si-peak for all the curves (CoK_α radiation).

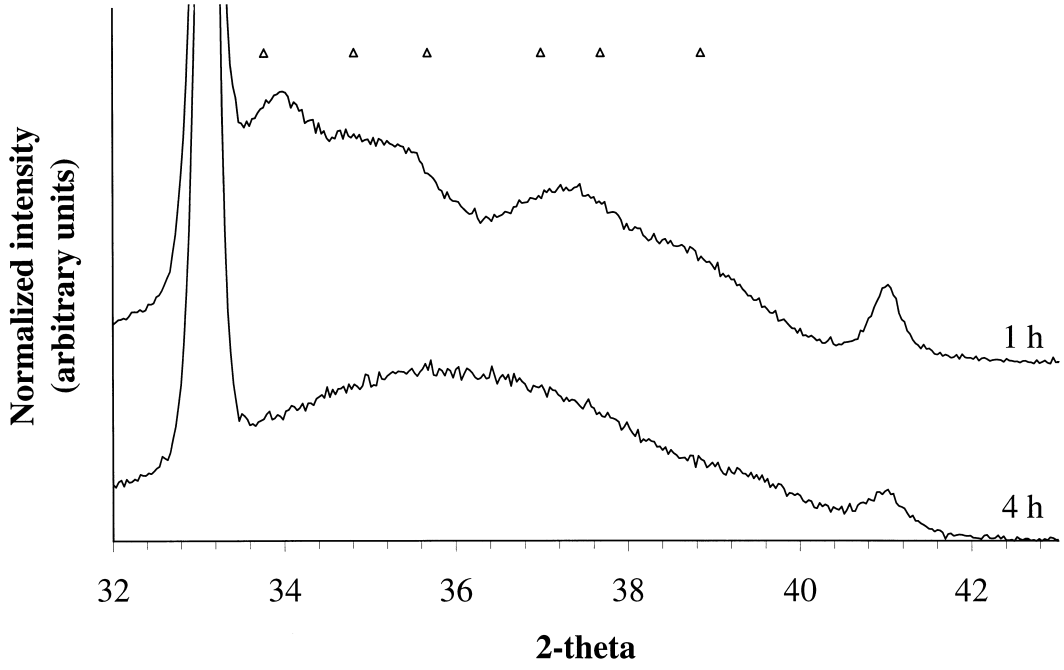

Fig. 3. XRD peaks of the transitory monoclinic yttria phase (CoK_α radiation). The angles of monoclinic yttria calculated from data in Gourlaouen et al.[16] are marked Δ.

milling time, while those of the Y_2A phase decrease at first to remain stable after more than 2 h of milling.

4. Discussion

Yttria has a cubic structure in its equilibrium form, but there are reports of it changing into a monoclinic form during milling with iron tools.[14] The new set of peaks that appeared after a short time of milling are not very clear, but as can be seen in Fig. 3, the agreement with the reported peaks of the monoclinic phase is reasonable.[15–17] This indicates that the yttria is first transformed to the monoclinic form before becoming amorphous. These steps are important during the subsequent heat-treatment of the milled powders since the

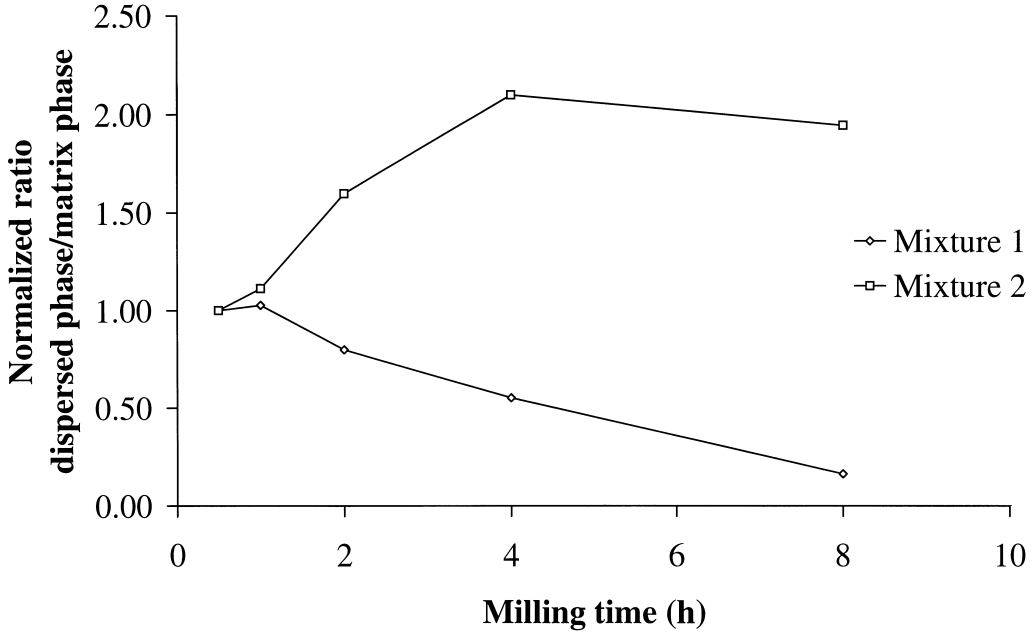

Fig. 4. Development of the dispersed phase to matrix phase ratio with the milling time. For mixture 1 an average of the selected peaks has been used.

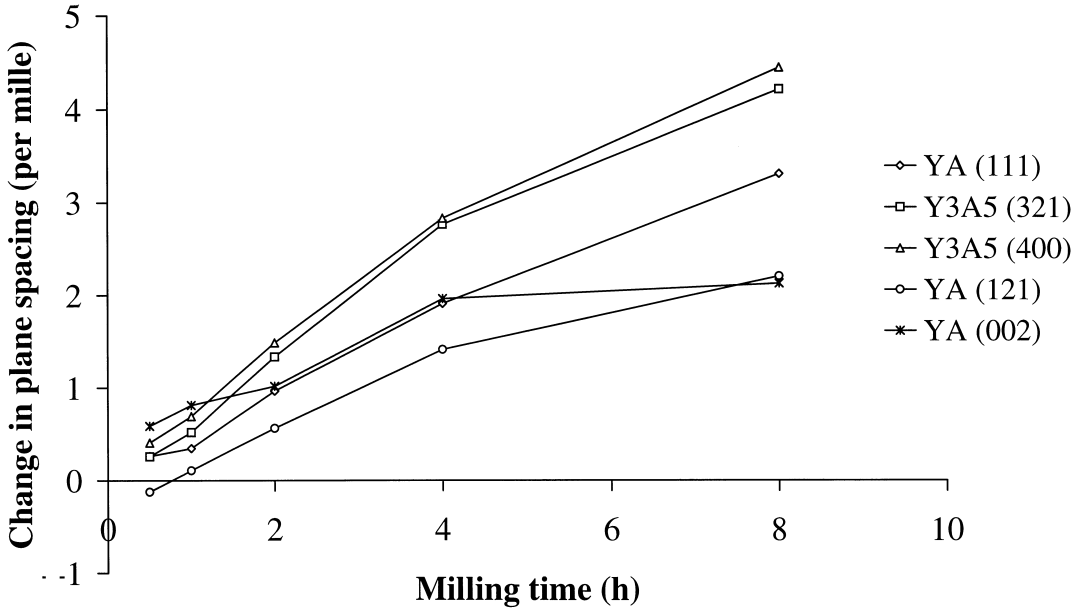

Fig. 5. Calculated change in plane spacing for mixture 1.

state of the yttria seems to be the factor deciding the route of the phase transformations in the sample. As long as it possesses a crystalline structure, the yttria prefers to return to the original cubic structure, and starts to do so even at quite low temperatures. On the other hand, if the yttria structure is completely broken up, the material remains amorphous up to 800°C, where the direct transformation to intermediate phases sets in. The latter reaction is quite sudden and exothermic, and can easily be seen in DTA. The results show that complete amorphization of the yttria is achieved between 2 and 4 h of milling.

Apart from the transitory formation of monoclinic yttria, the milling process does not seem to favor any formation of crystalline phases, such as for example the intermediate phases. Crystalline Y_3A_5 has been reported to be destroyed by the milling process.[18]

A probable explanation of the milling-time dependence of the observed shift in the XRD-peaks for some of the intermediate phases is that Y_3A_5 and YA can

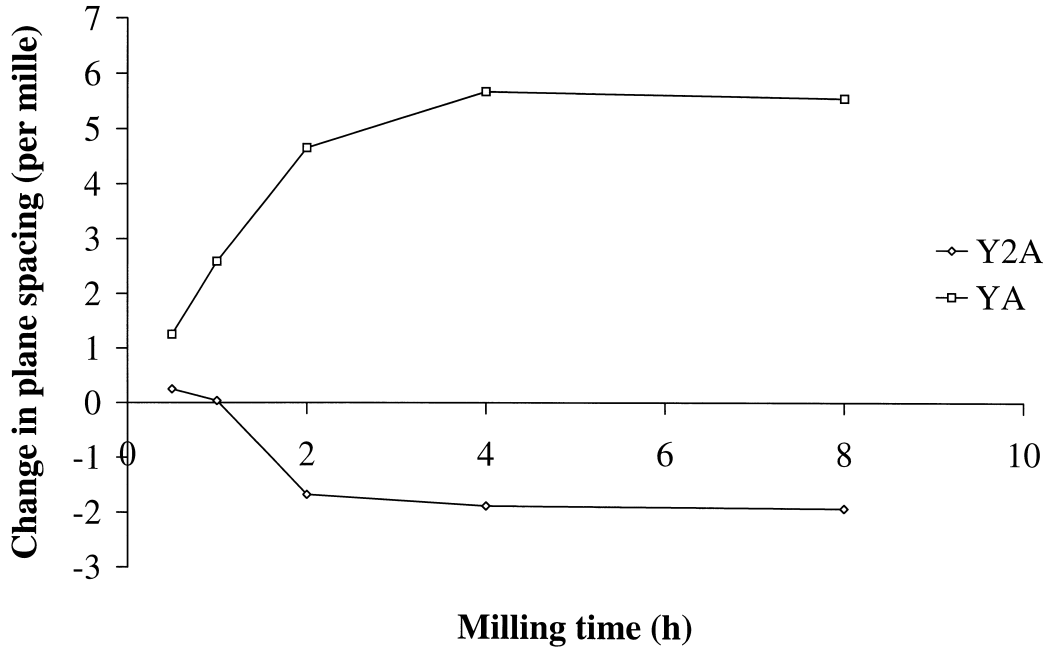

Fig. 6. Calculated change in plane spacing for mixture 2. The Y_2A plane is ($\bar{1}22$) and the YA plane is (200).

contain a substantial amount of Fe in solid solution picked up from the mill. Earlier work[19–21] reports complete interchangeability between Al and Fe for Y_3A_5 and extensive solubility for Al in $YFeO_3$. These reports, however, do not consider YA to be a stable phase. Later findings on the stability of YA[2,13] and our observations lead us to believe that there is also complete interchangeability of Fe and Al in YA. The Y_2A phase on the other hand is not expected to take up any iron, and the absence of a substantial shift in the calculated plane spacing does not contradict this.

Of the intermediate phases, Y_3A_5 is the most well known. Moreover its cubic structure makes observations regarding the lattice parameters easier than for the other phases. When subjected to iron contamination in an oxidizing environment (giving an addition of Fe_2O_3), the cell parameter changes with x according to

$$a = 12.37375 - 0.06502x - 0.00175x^2 \text{ Å}$$

for $Y_3Fe_{(5-x)}Al_xO_{12}$.[22–24] According to Strocka et al.[22] this polynomial lies within 0.006 Å of the data points used for the curve fit and provides an overall accuracy to within ±0.01 Å. On the basis of this and the plane spacings observed here, the amount of aluminum atoms replaced by iron can be estimated as 2, 3, 5, 9 and 14% for 0.5, 1, 2, 4 and 8 h of milling respectively. Given the estimated accuracy of the polynomial, the percentage of iron could be expected to be correct within a 2.5% margin.

This iron content in the Y_3A_5 phase would correspond to 9 wt% Fe_2O_3 after 8 h of milling. Looking at the ternary Fe_2O_3–Y_2O_3–Al_2O_3 phase diagram in Fig. 7,[19–21] Y_3A_5 is the dominant phase in mixture 1 and becomes even more so after the addition of Fe_2O_3. Therefore, the overall iron content can be expected to be roughly the same as the iron content of this phase. Considering the similar conditions during the milling of mixtures 1 and 2, there is reason to believe that the amount of iron pick-up in both mixtures does not differ much. A linear fit estimates that the addition of Fe_2O_3 is 1.4% of the original sample weight for every hour of milling under the given conditions. The above figures correspond reasonably well to the measured weight-loss of the milling media.

The observed shift in the ratio between phases with milling time (Fig. 4) agrees well with what is expected from an addition of oxidized iron to the system. Plotting the changes in the ternary phase diagram shows that in mixture 1 the amount of Y_3A_5 should increase at the expense of YA, and in mixture 2 the amount of YA should increase at the expense of Y_2A. This offers a method of easily controlling the ratio of phases within the sample. Considering the cost of milling equipment, it is a great advantage to be able to mill the powder mixture, and control the phase ratio, with steel tools instead of other materials such as alumina.

5. Conclusions

Mechanical alloying yttria-alumina mixtures accelerates attainment of equilibrium during subsequent heat treatment. In this respect relatively short milling times

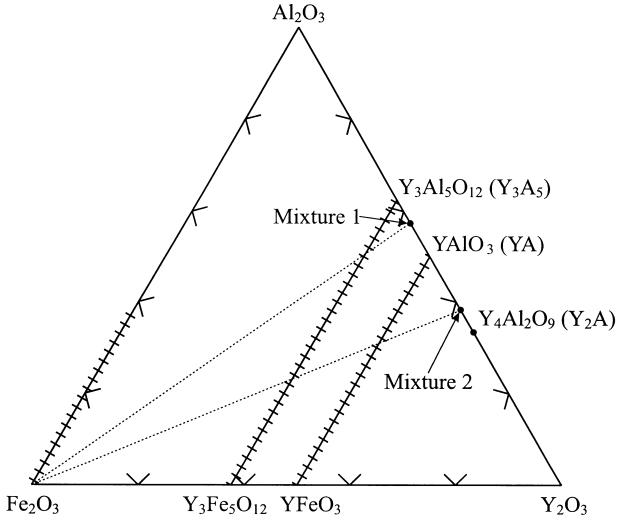

Fig. 7. Simplified ternary diagram after Van Hook.[20] Hatched lines denote solid solution, and the dotted lines the change of the mixtures when subjected to iron contamination. The $YFeO_3$–$YAlO_3$ solid solution has been prolonged all the way to the alumina–yttria binary line according to the conclusions in the text.

are sufficient to attain equilibrium during moderate heat treatment. However, the reaction path is affected by the milled state of the yttria. Milling can be used to introduce controlled amounts of Fe into the oxide phases.

References

1. Thompson, A. M., Chan, H. M. and Harmer, M. P., Tensile creep of alumina-silicon carbide 'nanocomposites'. *J. Am. Ceram. Soc.*, 1997, **80**(9), 2221–2228.
2. Cockayne, B., The uses and enigmas of the Al_2O_3–Y_2O_3 phase system. *J. Less-Common Metals*, 1985, **114**, 199–206.
3. Gaffet, E., Michel, D., Mazerolles, L. and Berthet, P., Effects of high energy ball milling on ceramic oxides. *Materials Science Forum*, 1997, **235–238**, 103–108.
4. Hay, R. S., Phase transformations and microstructure evolution in sol-gel derived yttrium–aluminum garnet films. *J. Mater. Res.*, 1993, **8**(3), 578–604.
5. Lakiza, S. M. and Lopato, L. M., Stable and metastable phase relations in the system alumina–zirconia–yttria. *J. Am. Ceram. Soc.*, 1997, **80**, 893–902.
6. Cockayne, B. and Lent, B., A complexity in the solidification behavior of molten $Y_3Al_5O_{12}$. *J. Crystal Growth*, 1979, **46**, 371–378.
7. Class, W., Growth of yttrium aluminate and yttrium aluminate garnet by a hollow cathode floating-zone method. *J. Crystal Growth*, 1968, **3–4**, 241–245.
8. Caslavsky, J. L. and Viechnicki, D. J., Melting behaviour and metastability of yttrium aluminum garnet (YAG) and $YAlO_3$ determined by optical differential thermal analysis. *J. Mater. Sci.*, 1980, **15**, 1709–1718.
9. Yamane, H., Omori, M., Okubo, A. and Hirai, T., High-temperature phase transition of $Y_4Al_2O_9$. *J. Am. Ceram. Soc.*, 1993, **76**(9), 2382–2384.
10. Abell, J. S., Harris, I. R., Cockayne, B. and Lent, B., An investigation of phase stability in the Y_2O_3–Al_2O_3 system. *J. Mater. Sci.*, 1974, **9**, 527–537.
11. Adylov, G. T., Voronov, G. V., Mansurova, E. P., Sigalov, L. M. and Urazaeva, E. M., The Y_2O_3–Al_2O_3 system above 1473 K. *Russ. J. Inorg. Chem.*, 1988, **33**(7), 1062–1067.
12. Mah, T. and Petry, M. D., Eutectic composition in the pseudobinary of $Y_4Al_2O_9$ and Y_2O_3. *J. Am. Ceram. Soc.*, 1992, **75**(7), 2006–2009.
13. Mah, T., Keller, K. A., Sambasivan, S. and Kerans, R. J., High-temperature environmental stability of the compounds in the Al_2O_3–Y_2O_3 system. *J. Am. Ceram. Soc.*, 1997, **80**(4), 874–878.
14. Begin-Colin, S., Le Caër, G., Zandona, M., Bouzy, E. and Malaman, B., Influence of the nature of milling media on phase transformations induced by grinding in some oxides. *J. Alloys and Compounds*, 1995, **227**, 157–166.
15. Hoekstra, H. R., Phase relationships in the rare earth sesquioxides at high pressure. *Inorg. Chem.*, 1966, **5**, 754–757.
16. Gourlaouen, V., Schnedecker, G., Lejus, A. M., Boncoeur, M. and Collongues, R., Metastable phases in yttrium oxide plasma spray deposits and their effect on coating properties. *Mater. Res. Bull.*, 1993, **28**, 415–425.
17. McPherson, R., Formation of metastable monoclinic rare earth sesquioxides from the melt. *J. Mater. Sci.*, 1983, **18**, 1341–1345.
18. Minkova, N. and Tzvetkov, G., Mechanochemical effects on yttrium–aluminum garnet. *Materials Letters*, 1998, **35**, 135–138.
19. Levin, E. M., Robbins, C. R. and McMurdie, H. F. (eds), *Phase Diagrams for Ceramists, Vol. II*. American Ceramic Society, Columbus, OH, 1969, pp. 56–57.
20. van Hook, H. J., Phase relations in the garnet region of the system Y_2O_3–Fe_2O_3–FeO–Al_2O_3. *J. Am. Ceram. Soc.*, 1963, **46**(3), 121–124.
21. MacChesney, J. B. and Potter, J. F., Phase relations applicable to the garnet phase $Y_3Fe_4AlO_{12}$. *J. Am. Ceram. Soc.*, 1965, **48**(10), 534–536.
22. Strocka, B., Holst, P. and Tolksdorf, W., An empirical formula for the calculation of lattice constants of oxide garnets based on substituted yttrium– and gadolinium–iron garnets. *Philips J. Res.*, 1978, **33**(3-4), 186–202.
23. Geller, S., Williams, H. J., Espinosa, G. P. and Sherwood, R. C., Importance of intrasublattice magnetic interactions and of substitutional ion type in the behavior of substituted yttrium iron garnets. *Bell. Syst. Tech. J.*, 1964, **43**(2), 565–623.
24. Gilleo, M. A. and Geller, S., Magnetic and crystallographic properties of yttrium–iron garnet, $3Y_2O_3{\cdot}xM_2O_3{\cdot}(5-x)Fe_2O_3$. *Phys. Rev.*, 1958, **110**, 73.